



HAL
open science

Kaposi's sarcoma-associated herpesvirus glycoprotein K8.1 is critical for infection in a cell-specific manner and functions at the attachment step on keratinocytes

Shanchuan Liu, Anna Großkopf, Xiaoliang Yang, Maximilian Erhard Mannheim, Marija Backovic, Stefano Scribano, Sarah Schlagowski, Armin Ensser, Alexander Hahn

► To cite this version:

Shanchuan Liu, Anna Großkopf, Xiaoliang Yang, Maximilian Erhard Mannheim, Marija Backovic, et al.. Kaposi's sarcoma-associated herpesvirus glycoprotein K8.1 is critical for infection in a cell-specific manner and functions at the attachment step on keratinocytes. *Journal of Virology*, 2023, 97 (10), pp.e0083223. 10.1128/jvi.00832-23 . pasteur-04130833

HAL Id: pasteur-04130833

<https://pasteur.hal.science/pasteur-04130833v1>

Submitted on 19 Jun 2023

HAL is a multi-disciplinary open access archive for the deposit and dissemination of scientific research documents, whether they are published or not. The documents may come from teaching and research institutions in France or abroad, or from public or private research centers.

L'archive ouverte pluridisciplinaire **HAL**, est destinée au dépôt et à la diffusion de documents scientifiques de niveau recherche, publiés ou non, émanant des établissements d'enseignement et de recherche français ou étrangers, des laboratoires publics ou privés.



Distributed under a Creative Commons Attribution - NonCommercial 4.0 International License

1 **Kaposi's sarcoma-associated herpesvirus glycoprotein K8.1 is critical for infection in a cell-**
2 **specific manner and functions at the attachment step on keratinocytes**

3

4 Shanchuan Liu^a, Anna K. Großkopf^{a, *}, Xiaoliang Yang^a, Maximilian Mannheim^b, Marija Backovic^b,
5 Stefano Scribano^a, Sarah Schlagowski^a, Armin Ensser^c, Alexander S. Hahn^{a#}

6

7 ^a Junior Research Group Herpesviruses, Infection Biology Unit, German Primate Center – Leibniz
8 Institute for Primate Research, Kellnerweg 4, 37077 Göttingen, Germany

9 ^b Institut Pasteur, Université Paris Cité, CNRS UMR3569, Unité de Virologie Structurale, 75015,
10 Paris, France

11 ^c Institute for Clinical and Molecular Virology, Friedrich-Alexander-Universität Erlangen-
12 Nürnberg, 91054 Erlangen, Germany

13 * present address: HIV & AIDS Malignancy Branch, Center for Cancer Research, National Cancer
14 Institute, Bethesda, Maryland, United States

15

16 Running Head: KSHV K8.1 mediates infection of skin keratinocytes

17

18

19 #Address correspondence to Alexander S. Hahn, ahahn@dpz.eu.

20

21

22

23 **ABSTRACT**

24 Kaposi's sarcoma-associated herpesvirus (KSHV) is associated with Kaposi's sarcoma and
25 B cell malignancies. K8.1, the major antigenic component of the KSHV virion, has been reported
26 to play a critical role in the infection of B cells, but otherwise its function remains enigmatic. We
27 created a K8.1 knockout virus (KSHVΔK8.1) in the BAC16 genetic background and analyzed its
28 infectivity on a range of adherent cells. We observed a strong defect on several epithelial cells,
29 e.g. the HaCaT keratinocyte cell line, HEK 293T and A549 lung epithelial cells, but no such defect
30 on other cells, among them e.g. lymphatic and blood endothelial cells. Mechanistically, we
31 found that reduced infectivity of the K8.1 knockout virus correlated with reduced attachment to
32 HaCaT cells. The defect in infectivity of KSHVΔK8.1 could be rescued by complementation
33 through expression of K8.1 in KSHVΔK8.1 producing cells by means of a lentiviral vector. In a
34 coculture infection model with iSLK producer cells, KSHVΔK8.1 was highly efficient at infecting
35 the BJAB B cell line but was significantly impaired at infecting the MC116 B cell line, in line with
36 a previous report. In fusion assays together with the gH/gL glycoprotein complex and gB, the
37 components of the conserved herpesviral core fusion machinery, we did not observe activation
38 of membrane fusion by K8.1 or its R8.1 homolog of the rhesus monkey rhadinovirus. In
39 summary, we found K8.1 to function in a highly cell-specific manner during KSHV entry at the
40 attachment step, playing an important role in the infection of epithelial cells.

41

42 **IMPORTANCE**

43 KSHV is the causative agent of several B cell malignancies and Kaposi's sarcoma. We
44 analyzed the function of K8.1, the major antigenic component of the KSHV virion, in the
45 infection of different cells. To do this, we deleted K8.1 from the viral genome. It was found that
46 K8.1 is critical for the infection of certain epithelial cells, e.g. a skin model cell line, but not for

47 infection of many other cells. K8.1 was found to mediate attachment of the virus to cells where
48 it plays a role in infection. In contrast, we did not find K8.1 or a related protein from a closely
49 related monkey virus to activate fusion of the viral and cellular membranes, at least not under
50 the conditions tested. These findings suggest that K8.1 functions in a highly cell-specific manner
51 during KSHV entry, playing a crucial role in the attachment of KSHV to e.g. skin epithelial cells.

52

53 **INTRODUCTION**

54 KSHV is the etiological agent of Kaposi's sarcoma (KS) and is associated with at least two
55 B cell malignancies, primary effusion lymphoma and a variant of multicentric Castleman's
56 disease. An association with KSHV-positive diffuse large B cell lymphoma was also reported (1–
57 5). A recent report suggests association with osteosarcoma (6), and the virus is associated with
58 the so-called KSHV inflammatory cytokine syndrome (7). KSHV-associated malignancies
59 constitute a major disease burden in Sub-Saharan Africa and in immunocompromised
60 individuals worldwide, in particular in the context of HIV infection (reviewed in (8, 9)). In some
61 African countries KS is the cancer that is associated with both the highest morbidity and
62 mortality among all types of cancer (10). A vaccine to prevent either KSHV primary infection or
63 the development of KSHV-associated diseases would be highly desirable. For both approaches,
64 understanding the function of the individual glycoproteins at the different stages of KSHV entry
65 into specific host cells is critical to understand their role during host colonization of individual
66 tissues.

67 The roles of the individual glycoproteins (GPs) of KSHV during the different steps of the
68 entry process, attachment, endocytosis, and membrane fusion, have so far only been poorly
69 defined in the context of different types of host cells. Like other herpesviruses KSHV encodes

70 the glycoproteins gB, gH, and gL that together form the conserved core fusion machinery of the
71 herpesviruses (11). While gB is the fusion executor, the interaction of KSHV gB with integrins
72 through an RGD motif may rather contribute to attachment or endocytosis (12–15). The
73 interaction of gH/gL with receptors from the Eph family can trigger membrane fusion by the
74 core fusion machinery (16, 17), similar to what is observed with the related human Epstein-Barr
75 virus or the rhesus monkey rhadinovirus (RRV) (16, 18). This at least holds true within the
76 experimental limits of these reports as gB always had to be substituted for a gB of a related
77 virus, either EBV or RRV, due to KSHV gB's extremely low fusogenicity, which makes it
78 unsuitable for assays measuring cell-cell fusion. Engagement of Eph family receptors also
79 triggers endocytosis (19–21). The exact function and molecular interactions of a proposed
80 fusion receptor, xCT, which normally forms a complex with CD98, so far remain unclear, with
81 different reports claiming either a direct role in fusion or for post-entry gene expression (15,
82 22).

83 The role of KSHV glycoprotein K8.1, also termed K8.1A or gp35-37 (23), is not well
84 understood. It binds heparan sulfate (24) and is the major antigenic component of the KSHV
85 virion (23). A role of K8.1, that is independent from its binding to heparan sulfate, in the
86 infection of the MC116 B cell line as well as in the infection of primary tonsillar B cells has been
87 described (25). Otherwise, its function remains enigmatic. For example, it is not known whether
88 K8.1 plays a role in the fusion process, something that could be suspected due to its potential
89 positional homology to the gp42-encoding gene of EBV within the KSHV genome. EBV gp42
90 clearly functions as a trigger of fusion (26). This hypothesis is also supported by homology of a
91 promoter element directly upstream of KSHV K8.1, EBV gp42, and RF8.1 of the retroperitoneal
92 fibromatosis herpesvirus of macaques (27), which may hint at a conserved biological role, even

93 if a sequence homology is not readily detectable across the whole protein. Another question is
94 whether K8.1 only plays a role for infection of some B cell populations or also for infection of
95 other cell types. We therefore generated a K8.1 deletion mutant and analyzed its relative
96 infectivity on different primary cells and cell lines. We also investigated K8.1's contribution to
97 virus attachment and triggering of the fusion machinery.

98

99 **RESULTS**

100 **Deletion of K8.1 results in decreased infectivity on several cell lines of epithelial origin.**

101 Previously, a role for K8.1 in the infection of B cells was reported by Dollery et al. (25)
102 but a comprehensive analysis of infection in other cell types was not performed in that study.
103 We therefore constructed a K8.1 deletion mutant, with a mutation/deletion of the start codon
104 and signal peptide of K8.1. While probably not necessary for this *in vitro* study, the strategy of
105 introducing a larger deletion in the signal peptide region was chosen to make sure that no
106 alternative start codon can give rise to a functional protein and to prevent reversion, also e.g. in
107 an experimental animal host in future studies. The deletion in the K8.1 locus (Fig. 1A) resulted in
108 the complete absence of the typical staining pattern with anti-K8.1 antibody observed after
109 Western blot analysis of crude virus preparations (Fig. 1 B) obtained by centrifugation of cell
110 culture supernatant from iSLK cells that had been previously transfected to harbor BAC16 wt or
111 Δ K8.1 and were induced to enter the lytic cycle. Glycoprotein H (gH) was abundantly detected in
112 the virus preparation, as was the capsid protein product of ORF65. While ORF65 and gH seemed
113 slightly more abundant in the Δ K8.1 preparation, DNase-resistant genome copy numbers
114 released into the cell culture supernatant after induction of the lytic cycle were not significantly
115 different between wt and Δ K8.1 virus, even if the Δ K8.1 mutant trended lower in this

116 experiment (Fig. 1 C). The “smear-like” staining pattern of K8.1 (Fig. 1 B) almost certainly stems
117 from its mucin-like degree of O-glycosylation with 18 predicted O-glycosylation sites according
118 to NetOGlyc 4.0 prediction (28) and is consistent with previous studies (23, 29–31). We
119 separated recombinantly produced K8.1 ectodomain, which was purified from the cell culture
120 supernatant of transfected 293T cells, by size exclusion chromatography (Fig. 1 D) and analyzed
121 the different fractions by gel electrophoresis (Fig. 1 E). This demonstrated that the K8.1
122 ectodomain exhibits a broad molecular weight distribution range, consistent with highly
123 heterogenous glycosylation and compatible with the pattern observed in Western blot analysis
124 of virus preparations (Fig. 1 B).

125 We next compared wt and Δ K8.1 virus on a range of different cell lines and primary cells
126 (Fig. 2 A). While infection of the SLK cell line (a clear renal carcinoma cell line) (32), U2197 (a
127 histiocytoma cell line) (33), and of primary human foreskin fibroblasts (HFF), human umbilical
128 vein endothelial cells (HUVEC), and lymphatic endothelial cells (LEC) cells was comparable, the
129 Δ K8.1 virus exhibited a significant defect on 293T cells and on A549 cells. On HaCaT cells, the
130 defect was also very pronounced but due to the overall low susceptibility of HaCaT could only
131 be shown at higher MOI after spin infection. The discrepancy in susceptibility of HaCaT to
132 infection by wt and Δ K8.1 virus in comparison to SLK cells was also confirmed in separate
133 experiments with another pair of virus stocks (Fig. 2 B), and it was not dependent on e.g. the
134 calcium concentration in the culture medium, which reportedly controls differentiation of
135 HaCaT (34). KS is primarily a cutaneous tumor and skin keratinocytes are infected by KSHV, also
136 in the context of KS lesions (35–37). HaCaT are a model cell line for keratinized epithelia that
137 retain the features of primary skin keratinocytes (38).

138 In order to control for possible non-specific off-target effects on viral infectivity that may
139 result from our genetic manipulation of the K8.1 locus, we performed a reconstitution
140 experiment. iSLK cells harboring BAC16ΔK8.1 were transduced with either empty lentiviral
141 vector (control) or a lentiviral vector coding for Tandem-Strep-tagged K8.1. We then compared
142 infection by KSHV wt or KSHVΔ8.1 produced from cells either transduced with empty lentiviral
143 vector or with lentiviral vector encoding K8.1. Infectivity of KSHVΔK8.1 on HaCaT, A549 and
144 293T cells was visibly rescued by reconstitution of K8.1 expression (Fig. 3 A). Calculation of the
145 50% infectious titer for each virus preparation (Fig. 3 B) from the data in Fig. 3 A demonstrated
146 that the reconstituted knockout virus did not differ significantly from KSHV wt with regard to
147 infectivity, while mock-reconstituted virus did. It should be noted that lentiviral transduction
148 may not lead to uniform expression of the transgene in all cells to the same degree and may be
149 limited with regard to the achievable expression levels, which likely precludes complete
150 reconstitution, as K8.1 is expressed to high levels during lytic KSHV replication. K8.1 expression
151 levels in virus preparations from K8.1-reconstituted KSHVΔK8.1-producing iSLK were similar to
152 expression levels in the wt virus preparation (Fig. 3 C).

153 **Deletion of K8.1 results in reduced cell-to-cell transmission into the MC116 B cell line**
154 **but not into the BJAB or Raji B cell lines**

155 Our previous work demonstrated that the BJAB B cell line is infected in a manner that is
156 highly dependent on the EphA7 receptor and to a lesser degree on the EphA5 receptor, and that
157 both receptors are engaged by the KSHV gH/gL complex, similar to the interaction with the high-
158 affinity EphA2 receptor (39). Work by Dollery and colleagues has demonstrated a critical role of
159 K8.1 for the infection of the MC116 B cell line (25), an EBV-negative Burkitt lymphoma cell line
160 (40, 41). We compared infection of MC116, BJAB, an EBV-negative Burkitt lymphoma cell line

161 (42), and Raji, an EBV-positive Burkitt lymphoma cell line (43, 44). Neither of the three cell lines
162 in our hands supported infection with free KSHV wt at levels exceeding 1% infected cells under
163 conditions that resulted in over 90% infected SLK cells (Fig. 4 A), which disagrees with previous
164 results for MC116 (45) but may be rooted in e.g. different culture conditions that lead to
165 differences in susceptibility. It should be noted that this time, we managed to achieve some
166 very low-level detectable infection of BJAB, unlike in earlier studies by our lab (39) and others
167 (46), suggesting that these cell lines may indeed vary in their susceptibility to some degree
168 across passages and subtle changes in culture conditions. Nevertheless, we could not compare
169 KSHV wt and Δ K8.1 as free virus and instead compared the two viruses on these cell lines head
170 to head in our established cell-to-cell transmission model for KSHV into B cell lines (39) that
171 roughly follows the established protocol by Myoung et al. (46), who first described the critical
172 role of cell-to-cell transmission for infection of lymphoblastoid B cell lines. We found that in
173 agreement with Dollery et al. (25) MC116 infection was highly dependent on K8.1, even if
174 MC116 in our hands exhibited comparatively low susceptibility (Fig. 4 B middle column pair). On
175 the other hand, infection of BJAB or Raji was completely independent of K8.1 (Fig. 4 B left and
176 right column pairs), again demonstrating that the deletion in KSHV Δ K8.1 does not cause a
177 general defect in infectivity or induction of the lytic cycle in these cell lines but instead causes a
178 highly cell-specific defect.

179 **Deletion of K8.1 results in reduced attachment to HaCaT skin epithelial cells.**

180 The defect in infectivity that was observed with KSHV Δ K8.1 on A549, 293T and
181 particularly HaCaT cells could conceivably be caused at different stages. As K8.1 is a
182 glycoprotein, the attachment step, endocytosis of the virus particle or fusion of viral and cellular
183 membranes come to mind. We analyzed attachment by replicating the spin infection protocol

184 used for the infection assay but immediately after centrifugation at 4° C, the cells were washed
185 with cold PBS and then harvested for quantification of cell-associated, DNase-resistant viral
186 nucleic acid as a surrogate marker for attachment. We found that attachment of KSHVΔK8.1 to
187 HaCaT cells was clearly and significantly reduced by over twofold in comparison to attachment
188 of KSHV wt (Fig. 5 A). Attachment to A549 and 293T cells was reduced as well, but to a lesser
189 degree, and the difference did not reach significance for 293T (which may reflect limitations of
190 the curve-fitting and statistical model, individual values at each concentration were clearly and
191 uniformly different).

192 **The importance of K8.1 for infection is partially reflected in its binding to cellular**
193 **membranes.**

194 In order to determine whether K8.1's function is related to its quantitative binding to the
195 membrane of target cells, which might mediate attachment, or rather an indirect effect of its
196 presence in the virion, we performed binding assays with a K8.1-Fc fusion protein that consists
197 of the extracellular domain of K8.1 fused to the Fc part of immunoglobulin G (Fig. 5 B).

198 For comparison, we also used similar molecules, gH-Fc/gL of KSHV that binds to heparan
199 sulfate and Eph family receptors (19, 47), and as control RRV gH-Fc mutated in the Plxdc1/2
200 receptor binding site and unable to bind Eph family receptors without gL (RRV gHΔ21-27-Fc)
201 (18), a molecule that in our hands does not bind to any cell tested so far. Binding of K8.1-Fc and
202 gH-Fc/gL to cell surfaces should mirror the availability of their respective receptors on these
203 cells, with the limitation that low-affinity interactions may be missed by such cellular binding
204 assays. It would be interesting to directly correlate K8.1's contribution to infection with the
205 expression levels of other known receptors, but the complexity of KSHV's interactions with
206 different Eph family members (17, 39, 48), integrin combinations (13, 15), lectins (49), and

207 heparan sulfate (24, 47), in addition to reported uncharacterized infection pathways (50),
208 precludes such a comparison. While we do not include gB, which currently is not available in its
209 trimeric pre-fusion form, differential binding of gH/gL and K8.1 might explain their relative
210 importance for infection and may represent a surrogate for comparing expression of their
211 respective receptors. Binding of K8.1-Fc measured as fold mean fluorescence intensity over
212 control was clearly most pronounced on 293T cells, followed by HaCaT, two cell lines where the
213 most pronounced defect of KSHV Δ K8.1 was observed. For HaCaT, in addition to high K8.1
214 binding, very low binding of gH-Fc/gL was observed, in line with low expression of EphA2 in this
215 cell line as reported by the human protein atlas (<https://www.proteinatlas.org/>). For A549, the
216 third cell line where KSHV Δ K8.1 showed a clear-cut defect, the picture was less clear. A549
217 exhibited K8.1 binding that was comparable to that on e.g. SLK or HFF and also interacted avidly
218 with gH-Fc/gL. Therefore, the relative importance of K8.1 for infection may be partially reflected
219 by the abundance of known cellular interaction partners like heparan sulfate proteoglycans or
220 of unknown interaction partners on the cell surface e.g. of HaCaT or 293T cells, but that does
221 not entirely explain its role, as exemplified by A549 cells, where neither K8.1 binding was
222 particularly pronounced nor gH/gL binding particularly low.

223 **Presence or absence of K8.1 or its RRV homolog does not appreciably modulate gH/gL-**
224 **activated membrane fusion by gB.**

225 While our results so far pointed to a function of K8.1 at the attachment step, mediating
226 binding of the virus to host cell membranes, a function in fusion is also possible. The EBV
227 glycoprotein gp42 for example, which is located at a similar or even the same position in the
228 EBV genome compared to K8.1 in the KSHV genome, triggers fusion (26). As KSHV gB is barely
229 fusogenic in cell-cell fusion assays, analyzing the trigger function of gH/gL on gB-mediated

230 membrane fusion is usually carried out using a gB from a related virus (17, 51). As established in
231 our group, we tested KSHV gH/gL together with gB of the related rhesus monkey rhadinovirus.
232 Addition of K8.1 to this combination of glycoproteins did not result in an increase in fusion of
233 effector cells expressing gH/gL/gB or gH/gB (Fig. 6 A). We tested fusion activity with and without
234 gL, which results in the ability or inability to use Eph family receptors for fusion (52). This
235 approach might demonstrate modulation of fusion that might be masked by Eph-mediated
236 membrane fusion in the presence of the full gH/gL complex. Even so, under none of these
237 conditions did K8.1 modulate fusion activity. As this only demonstrates a lack of action on
238 gH/gL-mediated fusion and due to the heterologous gB in the assay, direct activation of gB by
239 K8.1 might be impaired without any obvious effect in our assay if one postulates that R8.1 may
240 not interact with KSHV gB as K8.1 does. We therefore tested the positional homolog R8.1 of the
241 related RRV together with its cognate gH/gL, and gB. Similar to our results with KSHV K8.1, we
242 did not observe appreciable activation of cell-cell fusion on a range of different target cells by
243 RRV R8.1 (Fig. 6 B).

244

245 **DISCUSSION**

246 Taken together, our results demonstrate that in addition to the known function of K8.1
247 in the infection of B cells it has a critical function in the infection of epithelial cells, as observed
248 here for A549, 293T, and the skin model HaCaT cell line, which is not-derived from a tumor but
249 from a spontaneous immortalization event of cultured skin cells and is regarded as highly
250 representative of skin epithelium (38, 53). The specificity of the Δ K8.1 phenotype for certain
251 cells is striking as the K8.1 deletion had absolutely no effect on the infectivity of KSHV on
252 primary fibroblasts, primary endothelial cells and on the SLK and U2197 cell lines. The lack of a

253 phenotype of KSHVΔK8.1 on primary endothelial cells is in agreement with a previous report on
254 the function of K8.1 (25).

255 While we found a clear correlation of the K8.1 deletion with reduced attachment as
256 demonstrated for HaCaT cells (Fig. 5 A), we also found reduced infection of MC116 cells in a cell-
257 to-cell transmission setting, but normal infection of BJAB cells and Raji cells in this setting (Fig. 4
258 B). This would be compatible with the findings by Dollery et al., who described inhibition of
259 infection of primary tonsillar B cells by K8.1-targeting antibodies but could not achieve a
260 complete block, unlike as with MC116 cells (25), suggestive of both K8.1-dependent and K8.1-
261 independent infection also in primary B cell preparations. These previous findings and the
262 difference between the BJAB, Raji, and MC116 cell lines argue for the existence of more than
263 one single mechanism for the infection of B cells, which constitute a diverse population.

264 Our findings in the cell-to-cell transmission setting also suggest a function of K8.1 that
265 goes beyond the canonical concept of attachment as cell-to-cell transmission is believed to
266 function through some form of transfer of infectious virus from one cell to the other or even
267 through a so-called virological synapse, which conceivably might obviate the need for the virus
268 to attach to the target cell, even if that is so far speculation for KSHV. Nevertheless, this notion
269 would fit with the report by Dollery et al. that K8.1's function for infection of MC116 is
270 independent of heparan sulfate binding (25), which is generally believed to play a role for
271 attachment of viruses to cell membranes. On the other hand, we so far have no indication that
272 K8.1 or its close homologue, R8.1 of RRV, can trigger the core fusion machinery. Therefore, the
273 exact mechanism how K8.1 drives infection remains to be further elucidated. There is also the
274 possibility that while attachment in the original sense is not required during cell-to-cell
275 transmission, the "hand-over" of virus from one cell to the other still requires strong binding to

276 the target cell. In light of our results and previous reports (24, 25), it is conceivable that K8.1
277 acts through both its interaction with heparan sulfate proteoglycans and through additional
278 interactions that may play a comparatively more important role during infection of B cells. It
279 should also be noted that heparan sulfate proteoglycans contain a highly complex mixture of
280 sulfated sugars that may differ between cells (reviewed in (54)) and that the preferred heparan
281 sulfate moieties can be quite specific, as was also observed for gH of KSHV (47).

282 K8.1 may not only mediate attachment to epithelial cells but also aid in endocytosis of
283 the virus e.g. into MC116 cells, which would be compatible with our findings in adherent cells
284 and in the cell-to-cell transmission model for B cell lines. In line with this notion, Dollery et al.
285 did not observe reduced attachment to MC116 cells upon treatment of the virus with antibodies
286 directed to K8.1 (25). In a similar vein, the observed reduction in infectivity with KSHV Δ K8.1 for
287 293T and A549 (Figs 2 and 3) considerably exceeded the reduction in attachment observed
288 upon deletion of K8.1 (Fig. 5 A). In both scenarios, K8.1 would function more analogous to EBV
289 gp350, which mediates binding and endocytosis, particularly during B cell infection (55), than to
290 EBV gp42, which triggers membrane fusion (26).

291 In summary, we not only confirm K8.1's role for the infection of B cells as exemplified by
292 the MC116 line, but we also demonstrate a critical function during infection of several epithelial
293 cells, among them skin-derived keratinocytes. Ultimately, animal experiments will be needed to
294 faithfully elucidate the role of individual glycoproteins for cellular tropism and establishment of
295 persistent infection. With regard to the development of a glycoprotein-based KSHV vaccine, our
296 results argue for the inclusion of K8.1 in such an approach as K8.1 clearly functions during
297 infection of B cells and of skin-derived keratinocytes. Skin keratinocytes have previously been
298 reported to be susceptible to KSHV and to undergo a certain degree of immortalization through

299 infection (36), and skin is an organ that is prominently affected by KS (8). Epidermal
300 keratinocytes were shown to express cyclin D mRNA in cutaneous KS lesions (35) and were
301 shown to be KSHV-infected in such lesions (37), indicating that keratinocytes are at least to
302 some degree involved in cutaneous KS. The role of cutaneous infection in KSHV transmission is
303 unclear. Overall, in light of our findings here and previous results (19, 39, 48), targeting the
304 gH/gL complex to block binding to Eph family receptors together with K8.1 to selectively inhibit
305 infection of certain B cell populations (25) and impair infection of epithelial cells might be a
306 good starting point for the design of vaccine antigens.

307

308 **MATERIAL AND METHODS**

309 **Cells**

310 SLK cells (NIH AIDS Research and Reference Reagent Program), A549 (laboratory of
311 Stefan Pöhlmann, German Primate Center-Leibniz Institute for Primate Research, Göttingen,
312 Germany), Human embryonic kidney (HEK) 293T cells (laboratory of Stefan Pöhlmann), HaCaT
313 human keratinocytes (RRID: CVCL_0038), human foreskin fibroblasts (HFF) (laboratory of Klaus
314 Korn, Universitätsklinikum Erlangen, Institute for Clinical and Molecular Virology, Erlangen,
315 Germany), U2197 (Leibniz Institute DSMZ-German Collection of Microorganisms and Cell
316 Cultures GmbH) were cultured in Dulbecco's Modified Eagle Medium (DMEM), high glucose,
317 GlutaMAX, 25mM HEPES (Thermo Fisher Scientific) supplemented with 10% fetal calf serum
318 (FCS) (Thermo Fisher Scientific), and 50µg/ml gentamicin (PAN Biotech) (D10 medium). For low
319 calcium conditions, DMEM high glucose without calcium was supplemented as above and
320 brought to 0.03 mmol calcium from a 2.5 M stock solution. iSLK Bac16 cells (56, 57) (a kind gift
321 of Jae Jung and Don Ganem) were maintained in DMEM supplemented with 10% FCS, 50µg/ml

322 gentamicin, 2.5µg/ml puromycin (InvivoGen), 250µg/ml G418 (Carl Roth) and 200ug/ml
323 hygromycin (InvivoGen). Human vascular endothelial cells (HUVEC) were maintained in standard
324 Endothelial Cell Growth Medium 2 (both PromoCell). Human lymphatic endothelial cells (LEC)
325 were maintained in Endothelial Cell Growth Medium MV 2 (both PromoCell). BJAB (Leibniz-
326 Institut DSMZ-Deutsche Sammlung von Mikroorganismen und Zellkulturen GmbH), Raji
327 (RRID:CVCL_0511, a kind gift from Jens Gruber) and MC116 (a kind gift from Frank Neipel) were
328 cultured in RPMI 1640 medium (Thermo Fisher Scientific) supplemented with 10% fetal calf
329 serum (FCS) and 50 g/ml gentamicin (R10 medium).

330

331 **Deletion of K8.1 in BAC16**

332 The KSHV K8.1 deletion mutant (KSHVΔK8.1) was generated using a two-step, markerless λ-red-
333 mediated BAC recombination strategy as described by Tischer et al. (58). KSHVΔK8.1 harbors a
334 mutation of the K8.1 start codon to CGG followed by a 59-nucleotide deletion resulting in an
335 additional frameshift. In short, the recombination cassette was generated from the pEPKanS
336 template by polymerase chain reaction (PCR) with Phusion High Fidelity DNA polymerase
337 (Thermo Fisher Scientific) using long oligonucleotides (Ultramers; purchased from Integrated
338 DNA Technologies (IDT)) (KSHV_K8.1Mut_F:

339 TAAAGGGACCGAAGTTAATCCCTTAATCCTCTGGGATTAATAACCCGGGGTGGCGTGCCATGCCAATTGT

340 CCCACGTATCGAGGATGACGACGATAAGTAGGG, KSHV_K8.1Mut_R:

341 CTCTTGCCAGAATCCCAAATGCGAACGATACGTGGGACAATTGGCATGGCAGCCACCCGGGTTATTAA

342 TCCAGAGGATCAACCAATTAACCAATTCTGATTAG). The recombination cassette was transformed

343 into BAC16-carrying *Escherichia coli* strain GS1783, followed by kanamycin selection, and

344 subsequent second recombination under 1% L(+)-arabinose (Sigma-Aldrich)-induced I-SceI

345 expression. Colonies were verified by PCR of the mutated region followed by sequence analysis
346 (Macrogen), pulsed-field gel electrophoresis and restriction fragment length polymorphism. For
347 this purpose, bacmid DNA was isolated by standard alkaline lysis from 5ml liquid cultures.
348 Subsequently, the integrity of bacmid DNA was analyzed by digestion with restriction
349 enzyme *Xho*I and separation in 0.8% PFGE agarose (Bio-Rad) gels and 0.5×TBE buffer by pulsed-
350 field gel electrophoresis at 6 V/cm, 120-degree field angle, switch time linearly ramped from 1s
351 to 5s over 16 h (CHEF DR III, Bio-Rad). Infectious KSHV recombinants were generated by
352 transfection of purified bacmid DNA (NucleoBond Xtra Midi (Macherey-Nagel)) into iSLK cells
353 using GenJet Ver. II (Signagen) according to manufacturer's instructions. After visible GFP
354 expression, selection was performed using 200 µg/ml hygromycin B (InvivoGen) until only GFP
355 positive cells remained. Lytic replication of KSHV-BAC16 was induced in D10 medium by addition
356 of 2.5mM sodium-butyrate and 1µg/ml doxycycline. Supernatant was harvested after the cell
357 monolayer was destroyed. The BAC sequence was verified by Illumina-based next generation
358 sequencing.

359

360 **Recombinant virus production and Western blot**

361 iSLK BAC16 wt or ΔK8.1 cells were transduced with lentivirus harboring K8.1
362 overexpressing vector. After selection by blasticidin (InvivoGen), cells were induced by 2.5 mM
363 sodium-butyrate and 1 µg/ml doxycycline for 3 days. After that, the produced virus was
364 harvested and subjected to Western blot analysis after concentration by centrifugation through
365 a 5% Optiprep cushion as described previously (59). Western blot analysis was performed as
366 described previously (59), ORF65 was detected using a cross-reactive mouse monoclonal
367 antibody to RRV ORF65 (a kind gift from Scott Wong). K8.1 was detected using monoclonal

368 antibody BS555 (60), a kind gift from Frank Neipel. gH was detected using custom-made
369 polyclonal rabbit antibodies raised against peptides derived from KSHV gH (Genscript).

370

371 **Plasmids**

372 The following plasmids were used in this study: pLenti CMV Blast DEST (706–1) (Ax203, a
373 gift from Eric Campeau & Paul Kaufman, Addgene plasmid #17451); K8.1-OneStrep (OneStrep
374 Tag: SAWSHQPFEKGGGSGGGSGGSAWSHQPFEK) in the Ax203 backbone (Ax336); pcDNA6aV5his
375 encoding KSHV gH (Ax607); pcDNA3.1 encoding codon optimized KHSVgL (Ax252);
376 pcDNA6aV5his encoding RRV gB (Ax223); VP16-Gal4 (Ax388)(61); The KSHV gH ectodomain
377 (amino acids 22 through 704) N-terminally fused to the murine IgGkappa signal peptide and C-
378 terminally fused to FcFcStrep (Strep tag: SAWSHQPFEKGGGSGGGSGGSSWSHQPFEK) (Ax207,
379 backbone based on the pAB61 vector as described by Birkmann et al. (24))(19); the K8.1
380 ectodomain (amino acid 1 through 196) fused to FcFcStrep in the same backbone as Ax207
381 (Ax250); RRV 26-95 N-terminally fused to the murine IgGkappa signal peptide and C-terminally
382 fused to FcFcStrep, same backbone as Ax207 (Ax176); RRV 26-95 R8.1 ectodomain (amino acid
383 26 through 237) N-terminally fused to the murine IgGkappa signal peptide and C-terminally
384 fused to FcFcStrep in the same backbone as Ax207 (Ax243); pLenti CMV Blast DEST encoding a
385 Gal4-driven TurboGFP-Luciferase fusion reporter gene (Ax526)(51).

386

387 **Infection assays and flow cytometry**

388 For infection assay, cells were plated at 25 000 cells/well in 96-well plates. 16h after
389 plating, the cells were infected with the indicated amounts of virus. For HaCaT cells, spin
390 infection was used. After adding the virus, HaCaT cells were centrifuged for 2 h at 800 g, 37°C

391 (spin-infection). 48 h post infection, the cells were harvested by brief trypsinization, followed by
392 adding 5% FCS in PBS to inhibit trypsin activity. Then, the cell suspension was transferred to an
393 equal volume of PBS supplemented with 4% methanol-free formaldehyde (Carl Roth) for
394 fixation. A minimum of 5 000 cells was analyzed per well for GFP expression on an ID7000
395 (Sony). The cell-to-cell transmission assay was based on our previous protocol (39), which in
396 turn was based on the work by Myoung et al.(46). Briefly, the whole coculture was stained with
397 anti-CD20 antibody conjugated to Alexa647 and with anti-CD13 antibody conjugated to PE. Only
398 the GFP-positive cells in the CD20-positive and CD13-negative population were evaluated in
399 order to separate the iSLK producer cells from B cell target cell lines.

400 50% infectious titers were calculated by non-linear regression using the “[Agonist] vs.
401 response – FindECanything” model with E constrained to 50 (for calculation of EC50), bottom to
402 0, and top to 100 (GraphPad Prism 9.4.1). The same model was used for curve fitting.

403

404 **Quantitative realtime-PCR-based viral genome copy number analysis**

405 Concentrated virus samples were treated with DNaseI (0.1 units/ μ l) to remove non-
406 encapsidated DNA (37°C, overnight). Subsequently, DNaseI was deactivated, and viral capsids
407 were disrupted by heating the sample to 95°C for 30 minutes. Realtime-PCR (qPCR) was
408 performed on a StepOne plus cycler (Thermo Fisher Scientific) in 20 μ l reactions using the Sensi
409 FAST Probe Hi-ROX Kit (Bioline) (cycling conditions: 3min in initial denaturation at 95°C, 40
410 cycles 95°C for 10s and 6°C for 35s). All primer-probe sets were purchased from IDT as complete
411 PrimeTime qPCR Assays (primer: probe ratio: 4:1). Samples were analyzed in technical
412 duplicates. A series of six 10-fold dilutions of bacmid DNA was used as the standard for absolute
413 quantification of viral genome copies based on qPCR of ORF59 of KSHV.

414 **Virus attachment assay**

415 HaCaT and SLK cells were seeded on the 12-well plate at 200 000 cells/well for virus
416 attachment. After adding indicated amount of virus, cells were centrifuged for 30min at 4122g
417 (4200rpm) at 4°C. After three washes with ice-cold PBS, genomic DNA was isolated using the
418 ISOLATE II Genomic DNA Kit (Bioline) according to the manufacturer's instructions. The amount
419 of viral DNA was determined by qPCR from equal amounts of extracted DNA. For some
420 experiments, relative values of bound viral genomes to cellular DNA were calculated based on
421 Δ Ct values for viral genomic loci (ORF59 for KSHV) and a cellular genomic locus (CCR5), yielding
422 equivalent results (not shown).

423

424 **Production of recombinant viral proteins**

425 Soluble K8.1-Fc, KSHV gH-Fc/gL, R8.1-Fc, and RRV gH Δ 21-27-Fc protein were purified by
426 Strep-Tactin chromatography from 293T cell culture supernatant. 293T cells were transfected by
427 Polyethylenimine "Max" (PEI) (Polysciences) transfection with the respective expression
428 plasmids. The protein-containing cell culture supernatant was passed over 0.5ml of a Strep-
429 Tactin Superflow (IBA Lifescience) matrix in a gravity flow Omniprep column (BioRad). Bound
430 protein was washed with approximately 50ml phosphate buffered saline pH 7.4 (PBS) and
431 eluted in 1ml fractions with 3mM desthiobiotin (Sigma-Aldrich) in PBS. Protein-containing
432 fractions were pooled, and buffer exchange to PBS via VivaSpin columns (Sartorius) was
433 performed. Protein concentration was determined by absorbance at 280nm. Aliquots were
434 frozen and stored at -80°C.

435 Soluble K8.1 ectodomain for size exclusion chromatography analysis was produced in
436 Expi293 (Thermo Fisher). The cells were transfected with a synthetic gene, codon optimized for

437 expression in mammalian cells and encoding glycoprotein K8.1 ectodomain (residues 1-194,
438 Uniprot O36551), which was cloned into the pCAGGs vector (62). The construct contained
439 endogenous K8.1 signal peptide to drive its secretion, and a C-terminal Twin-strep tag
440 (WSHPQFEKGGGSGGGSGGSSAWSHQPFEK) for affinity purification. For transfection, Expi293
441 cells were diluted to density of 2×10^6 cell/ml in FreeStyle Expi293 media (Thermo Fisher) the day
442 before transfection. One day later, the cells were centrifuged at 200 x g for 10 minutes at room
443 temperature, and resuspended in pre-warmed FreeStyle media to density of 3×10^6 cells/ml. The
444 resuspended cells were transfected with the expression plasmid using FectoPro transfection
445 agent (Polyplus) and 1 μ g of DNA per ml of cell culture, with 1:1 ratio of DNA (mg) per FectoPro
446 reagent (ml). Five days post-transfection, the supernatant was separated from the cells by
447 centrifugation at 3,000 x g for 10 minutes at 4°C. Secreted K8.1 was purified from the
448 supernatant on a Streptactin column (Cytiva) according to manufacturer's protocol. The affinity
449 purified K8.1 was concentrated to 0.3 ml and loaded onto the Superdex200 10/300 (Cytiva) size
450 exclusion column, using 10 mM Tris pH8, 50mM NaCl as a running buffer.

451

452 **Binding assays using recombinant viral proteins**

453 Cells were detached by 0.25M EDTA in PBS and transferred to the falcon tube at 200 000
454 cells/tube. After discarding the supernatant, cells were fixed in 2% methanol-free formaldehyde
455 (Carl Roth) for 10 min, followed by once washing with PBS. Subsequently, cells were blocked in
456 5% FCS in PBS for 1 h at 4°C and then incubated with 10 μ g/m proteins in 5% FCS in PBS for 1 h
457 at 4°C, followed by two washes with PBS and one wash with 5% FCS in PBS. Then, the cells were
458 incubated with Alexa Fluor® 647 anti-human Fc Antibody (Thermo Fisher Scientific) at a ratio of
459 1:200 for 45 min at 4°C in the dark, followed by three washes with PBS. Finally, the cells were

460 stored in 1% methanol-free formaldehyde in PBS until flow cytometry analysis on an ID7000
461 (Sony).

462

463 **Cell-cell fusion assay**

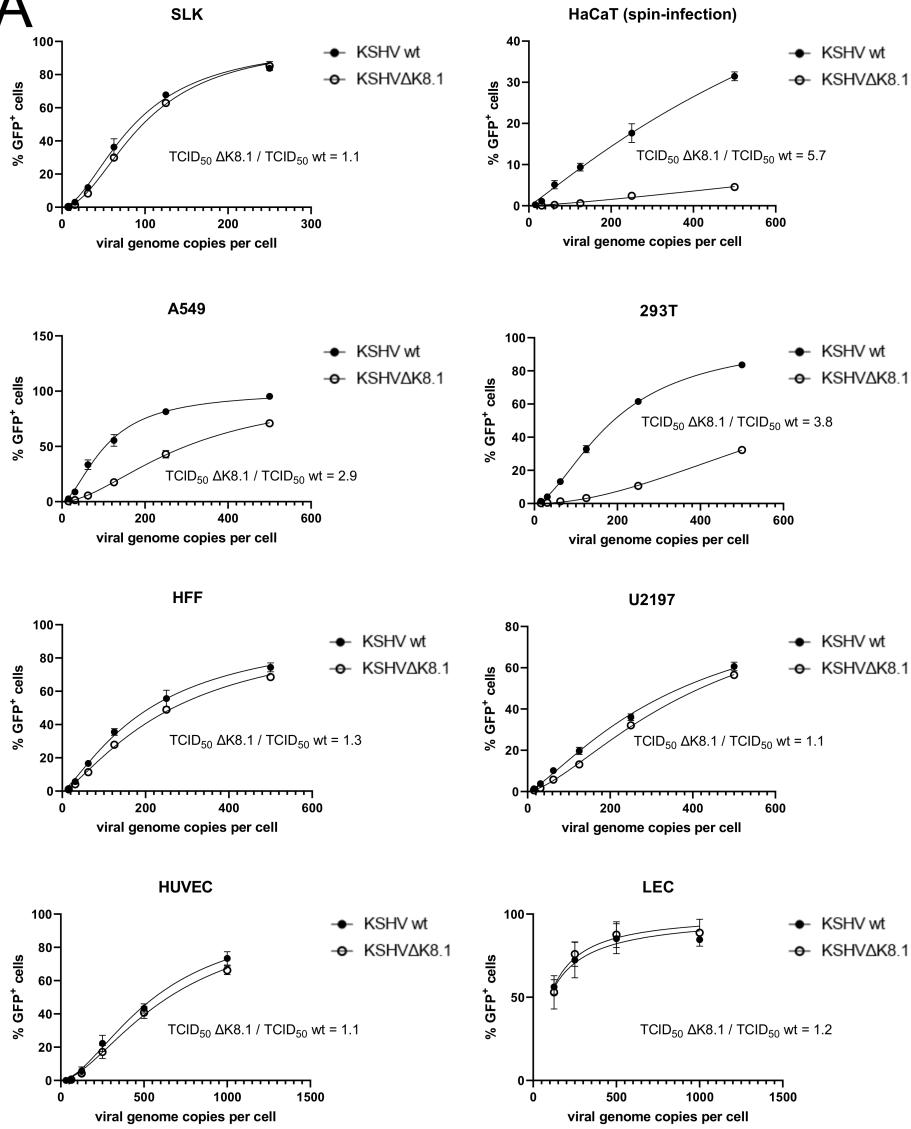
464 SLK, HaCaT, A549, 293T target cells were stably transduced with a lentiviral construct
465 encoding a Gal4 response element-driven TurboGFP-luciferase reporter (51) and fusion assays
466 were performed similar to as described previously (18, 51, 61). 293T effector cells were seeded
467 in 96-well plates at 30 000 cells/well. One day after, 293T effector cells were transfected with a
468 plasmid encoding the Gal4 DNA binding domain fused to the VP16 transactivator (VP16-Gal4),
469 and the indicated viral glycoprotein combinations or a pcDNA empty vector control (VP16-Gal4:
470 31.25 ng/well, K8.1: 25ng/well, KSHV gH: 12.5 ng/well, KSHV gL: 62.5ng/well, RRV gB: 18.75
471 ng/well, pcDNA only: 118.75 ng/well) using PEI as described before (51). 24 h after transfection,
472 the medium on 293T effector cells was removed entirely and exchanged to 100µl fresh D10. The
473 target cells were re-suspended and counted, and 40 000 target cells were added to 293T
474 effector cells in 100µl fresh D10. Triplicate wells were analyzed for all target-effector
475 combinations. After 48h, cells were washed once in PBS and lysed in 35 µl 1x Luciferase Cell
476 culture lysis buffer (E1531, Promega) for 15min at room temperature and centrifuged for 10min
477 at 4°C. 20 µl of each cell lysate was used to measure luciferase activity using the Beetle-Juice
478 Luciferase Assay (PJK) according to the manufacturer's instructions on a Biotek Synergy 2 plate
479 reader.

480

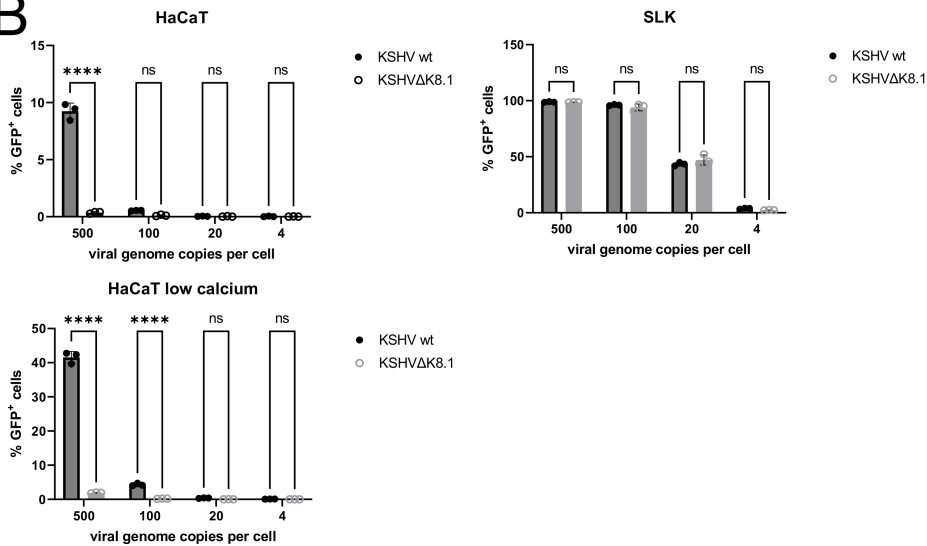
481 **FIGURE LEGENDS**

488 Size exclusion chromatography elution profile of purified K8.1 ectodomain, that was
489 recombinantly produced in Expi293 cells. E) Polyacrylamide gel electrophoresis of fractions (20
490 μ l per sample) from (D), stained with Coomassie blue.

A

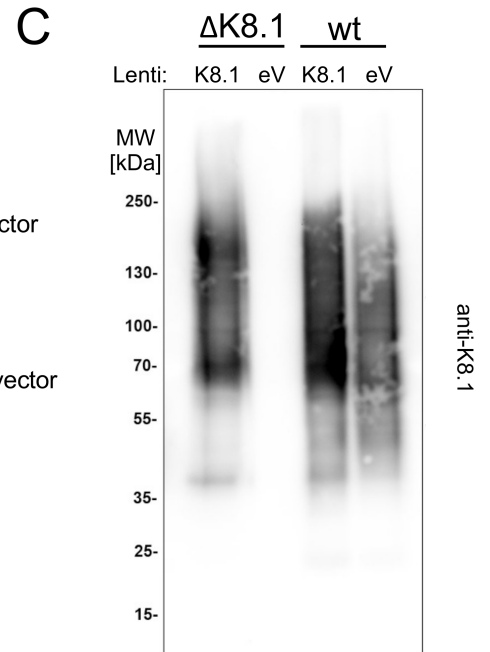
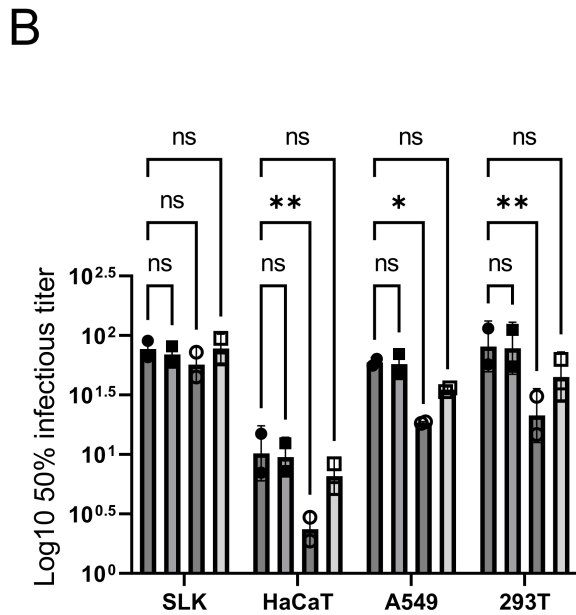
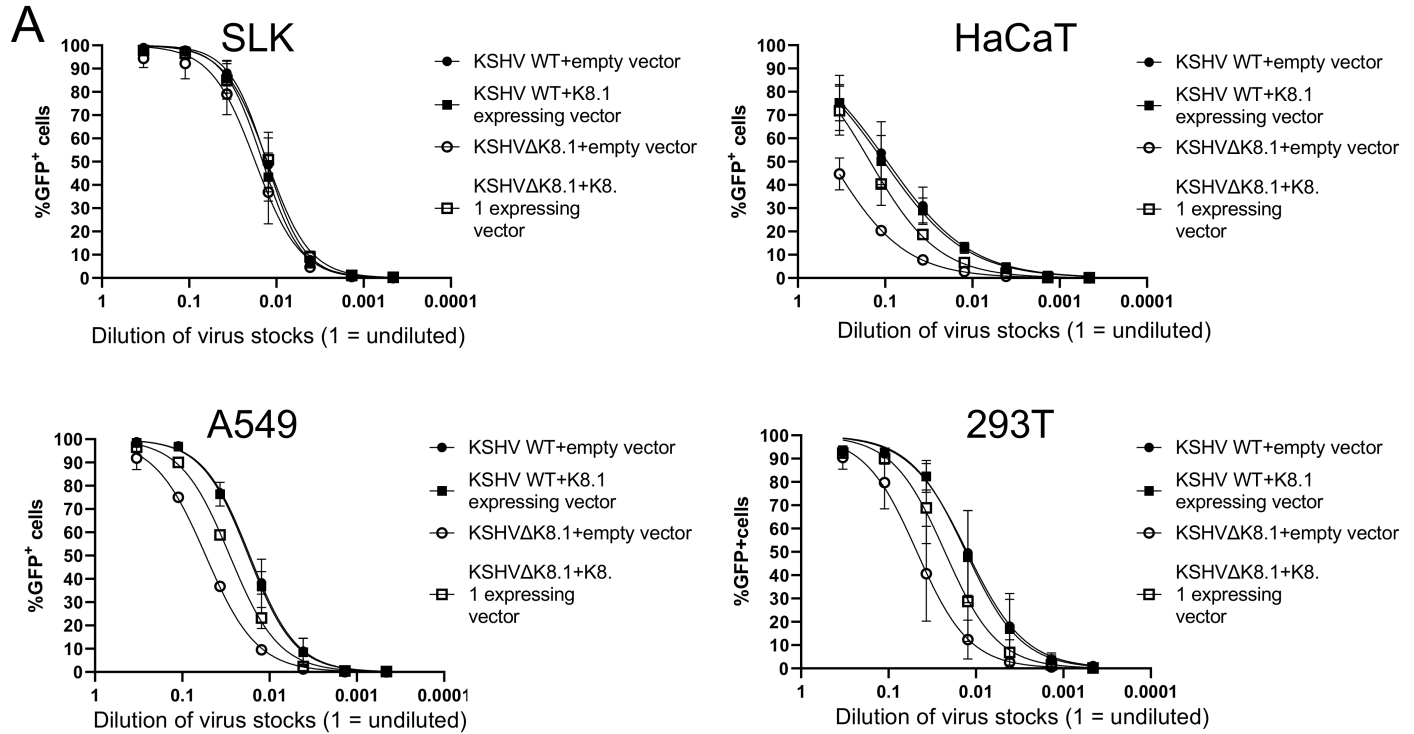


B



492 **Figure 2. Loss of K8.1 results in cell-specific defects in infectivity on different types of**
493 **adherent cells.** A) Different cell lines and primary cells were infected with BAC16-derived KSHV
494 wt or KSHV Δ K8.1 using the same number of virus particles as measured by DNase-resistant
495 genome copies. Infection was quantified by the percentage of GFP reporter gene-expressing
496 cells. One representative experiment of two independent experiments with two independent
497 pairs of virus stocks is shown. B) Repeat experiment comparing infection of SLK and HaCaT
498 (without spin-infection at normal cell culture conditions and at low calcium) by KSHV wt and
499 KSHV Δ K8.1. **** = $p < 0.0001$, ns = non-significant. Two-Way ANOVA with Sidak's correction for
500 multiple comparisons, $n=3$.

501



502

503

Figure 3. Recombinant K8.1 expression in virus producing cells reverts the cell-specific

504

defect in infectivity of KSHVΔK8.1. A) Infection of SLK, HaCaT, A549, and 293T. HaCaT were

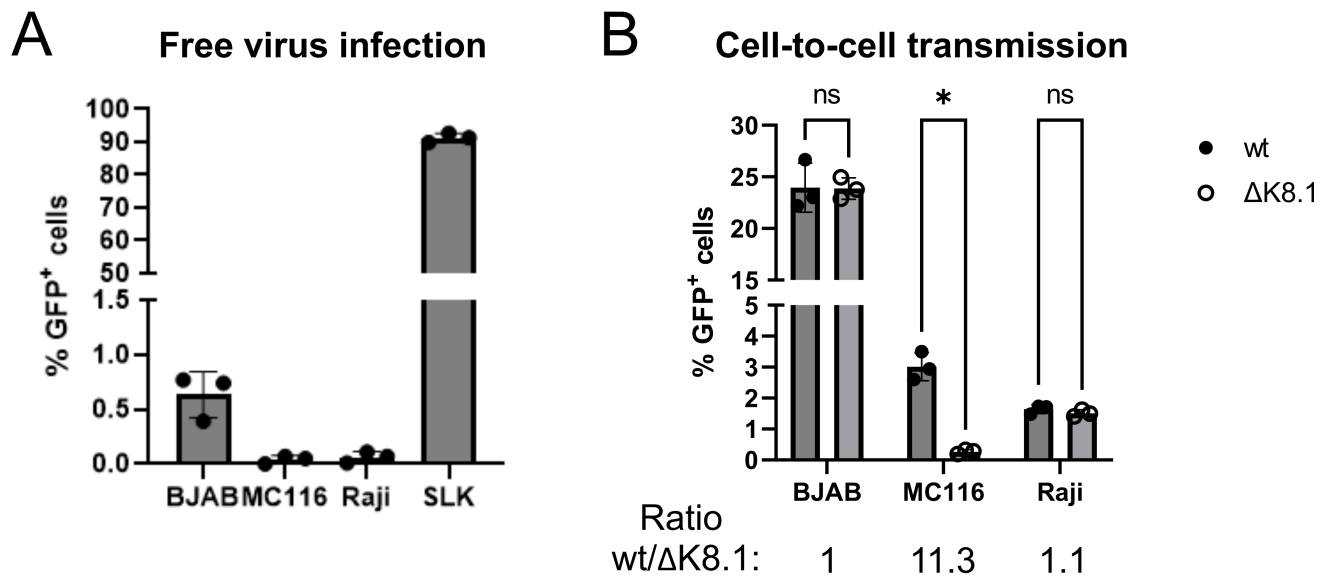
505

infected by spin-infection. Error bars represent the standard deviation of two experiments, each

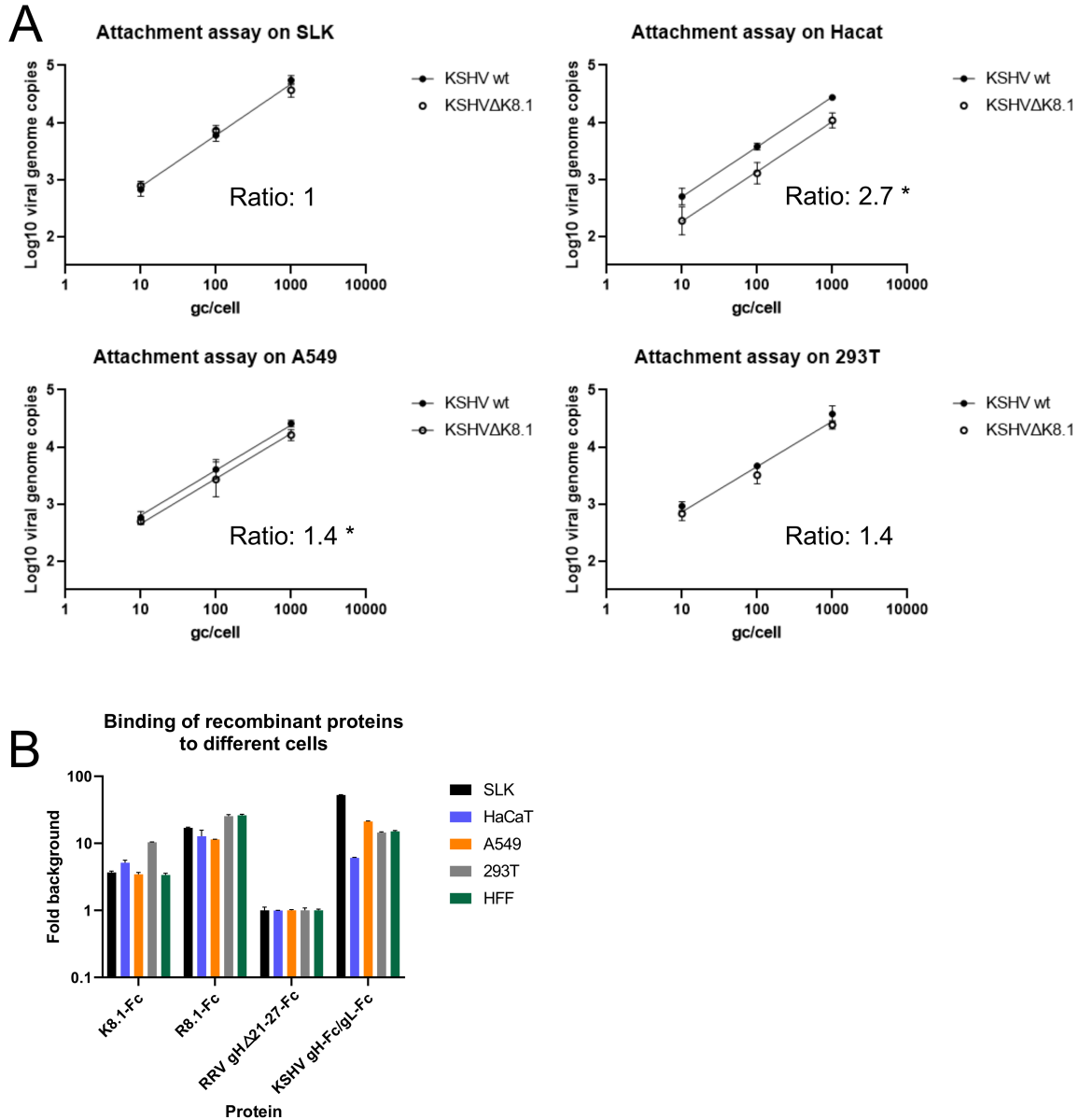
506

performed in triplicates. B) 50% infectious titers were calculated from the data in (A) using curve

507 fitting as described in the methods section for each of the two independent experiments, log-
 508 transformed, and analyzed by Two-Way ANOVA with Sidak's correction for multiple
 509 comparisons (n=2, * = p<0.05; ** = p<0.01. C) Western blot analysis of virus preparations from
 510 chemically induced iSLK producer cells harboring BAC16 KSHV Δ K8.1 or BAC16 KSHV wt,
 511 transduced with empty vector (eV) or a lentiviral vector coding for K8.1 tagged with a C-terminal
 512 tandem StrepTag (K8.1).
 513



514
 515 **Figure 4. KSHV Δ K8.1 exhibits a defect in cell-to-cell transmission into the MC116 B cell**
 516 **line.** A) Cell-free infection of B cell lines with KSHV is inefficient. Cell lines were infected with the
 517 same KSHV BAC16 wt virus stock under comparable conditions. B) iSLK cells carrying the BACs
 518 coding for the respective viruses were chemically induced to enter the lytic cycle and were co-
 519 cultured with the indicated target cells. Infection was determined after 4 days by flow
 520 cytometry. Error bars represent the standard deviation; * p<0.05, Two-Way ANOVA with Sidak's
 521 correction for multiple comparisons, n=3.



523

524

Figure 5. KSHVΔK8.1 exhibits reduced attachment on HaCaT cells. A) SLK, HaCaT, A549

525

or 293T cells were spin-infected at 4° C with the indicated amounts of virus and bound viral DNA

526

was quantified by qPCR. Binding curves for KSHV wt and KSHVΔK8.1 were indistinguishable on

527

SLK but significantly different for HaCaT and A549. (Non-linear fit for semi-log data by least

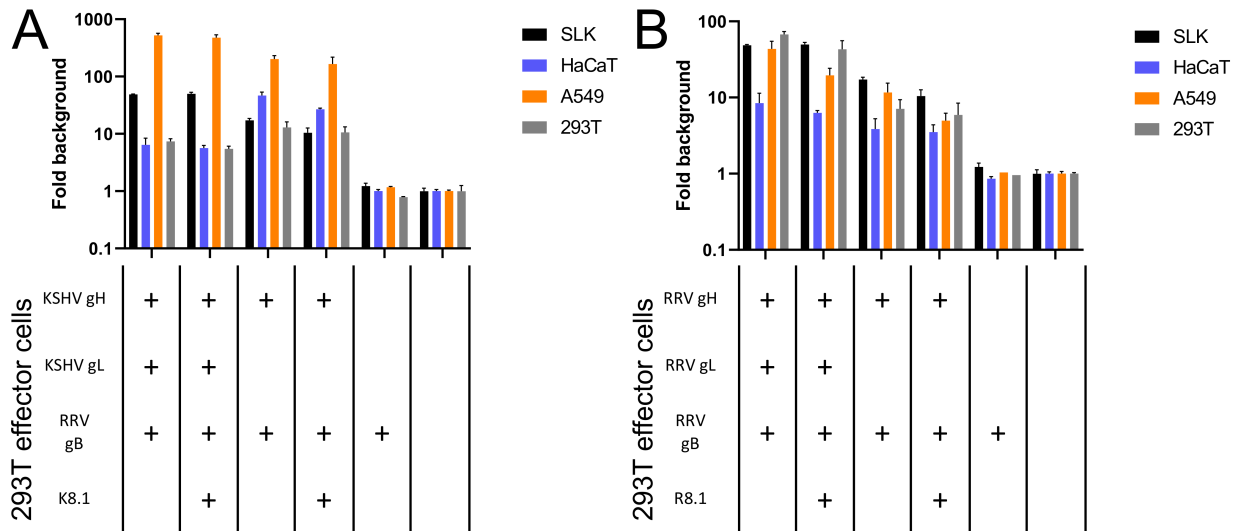
528

squares regression using mean values for each data point, slope shared between curves, ratio

529

calculated from Y-intercept; two curves and * indicate significant difference with p<0.05; n=6) B)

530 Binding of Fc-fusion proteins K8.1-Fc, gH-Fc/gL, R8.1-Fc or RRV gHΔ21-27-Fc
 531 (control/background) to the indicated cells was measured by flow cytometry. Error bars
 532 represent the standard deviation, n=3.
 533



534
 535 **Figure 6. Presence or absence of K8.1 or its RRV homolog do not appreciably modulate**
 536 **gH/gL-activated membrane fusion by gB.** A) KSHV gH/gL together with RRV gB or KSHV gH
 537 together with RRV gB were expressed in the presence or absence of K8.1 on 293T effector cells,
 538 and these cells were co-cultured with the indicated target cell populations. Error bars represent
 539 the standard deviation of triplicate samples. B) RRV gH/gL together with RRV gB or RRV gH
 540 together with RRV gB were expressed in the presence or absence of R8.1 on 293T effector cells,
 541 and these cells were co-cultured with the indicated target cell populations. Error bars represent
 542 the standard deviation of triplicate samples.

543
 544
 545 **ACKNOWLEDGEMENTS**

546 This work was supported by grants to ASH from the Deutsche Forschungsgemeinschaft
547 (www.dfg.de, HA 6013/4-1 and HA 6013/10-1) and from the Wilhelm-Sander-Foundation
548 (www.wilhelmsander-stiftung.de, project 2019.027.1). We would like to thank Frank Neipel,
549 Scott Wong, Klaus Korn, Jens Gruber, and Stefan Pöhlmann for sharing reagents and resources.
550 We thank Timothy Rose for helpful discussions.

551

552 **DECLARATION OF INTEREST**

553 The authors declare no competing interests. Alexander Hahn is also an employee of GSK, which
554 did not have any influence on this study.

555

556 **REFERENCES**

- 557 1. Cesarman E, Chang Y, Moore PS, Said JW, Knowles DM. 1995. Kaposi's sarcoma-
558 associated herpesvirus-like DNA sequences in AIDS-related body-cavity-based lymphomas. *N*
559 *Engl J Med* 332:1186–1191.
- 560 2. Chang Y, Cesarman E, Pessin MS, Lee F, Culpepper J, Knowles DM, Moore PS. 1994.
561 Identification of herpesvirus-like DNA sequences in AIDS-associated Kaposi's sarcoma. *Science*
562 266:1865–1869.
- 563 3. Parravicini C, Corbellino M, Paulli M, Magrini U, Lazzarino M, Moore PS, Chang Y.
564 1997. Expression of a virus-derived cytokine, KSHV vIL-6, in HIV-seronegative Castleman's
565 disease. *Am J Pathol* 151:1517–1522.
- 566 4. Soulier J, Grollet L, Oksenhendler E, Cacoub P, Cazals-Hatem D, Babinet P, d'Agay MF,
567 Clauvel JP, Raphael M, Degos L. 1995. Kaposi's sarcoma-associated herpesvirus-like DNA
568 sequences in multicentric Castleman's disease. *Blood* 86:1276–1280.
- 569 5. Wen KW, Wang L, Menke JR, Damania B. 2022. Cancers associated with human
570 gammaherpesviruses. *The FEBS Journal* 289:7631–7669.
- 571 6. Chen Q, Chen J, Li Y, Liu D, Zeng Y, Tian Z, Yunus A, Yang Y, Lu J, Song X, Yuan Y.
572 2021. Kaposi's sarcoma herpesvirus is associated with osteosarcoma in Xinjiang populations.
573 *PNAS* 118.
- 574 7. Goncalves PH, Ziegelbauer J, Uldrick TS, Yarchoan R. 2017. Kaposi sarcoma
575 herpesvirus-associated cancers and related diseases. *Current Opinion in HIV and AIDS* 12:47–56.
- 576 8. Cesarman E, Damania B, Krown SE, Martin J, Bower M, Whitby D. 2019. Kaposi
577 sarcoma. *Nat Rev Dis Primers* 5:1–21.
- 578 9. Yarchoan R, Uldrick TS. 2018. HIV-Associated Cancers and Related Diseases. *N Engl J*
579 *Med* 378:1029–1041.
- 580 10. Bray F, Ferlay J, Soerjomataram I, Siegel RL, Torre LA, Jemal A. 2018. Global cancer

581 statistics 2018: GLOBOCAN estimates of incidence and mortality worldwide for 36 cancers in
582 185 countries. *CA Cancer J Clin* <https://doi.org/10.3322/caac.21492>.

583 11. Connolly SA, Jardetzky TS, Longnecker R. 2021. The structural basis of herpesvirus
584 entry. *Nat Rev Microbiol* 19:110–121.

585 12. Garrigues HJ, DeMaster LK, Rubinchikova YE, Rose TM. 2014. KSHV attachment and
586 entry are dependent on $\alpha V\beta 3$ integrin localized to specific cell surface microdomains and do not
587 correlate with the presence of heparan sulfate. *Virology* 0:118–133.

588 13. Garrigues HJ, Rubinchikova YE, DiPersio CM, Rose TM. 2008. Integrin $\{\alpha\}V 3$
589 Binds to the RGD Motif of Glycoprotein B of Kaposi's Sarcoma-Associated Herpesvirus and
590 Functions as an RGD-Dependent Entry Receptor. *J Virol* 82:1570–1580.

591 14. Akula SM, Pramod NP, Wang F-Z, Chandran B. 2002. Integrin $\alpha 3\beta 1$ (CD 49c/29) Is a
592 Cellular Receptor for Kaposi's Sarcoma-Associated Herpesvirus (KSHV/HHV-8) Entry into the
593 Target Cells. *Cell* 108:407–419.

594 15. Veettil MV, Sadagopan S, Sharma-Walia N, Wang F-Z, Raghu H, Varga L, Chandran B.
595 2008. Kaposi's Sarcoma-Associated Herpesvirus Forms a Multimolecular Complex of Integrins
596 ($\alpha V\beta 5$, $\alpha V\beta 3$, and $\alpha 3\beta 1$) and CD98-xCT during Infection of Human Dermal Microvascular
597 Endothelial Cells, and CD98-xCT Is Essential for the Postentry Stage of Infection. *Journal of*
598 *Virology* 82:12126–12144.

599 16. Chen J, Sathiyamoorthy K, Zhang X, Schaller S, Perez White BE, Jardetzky TS,
600 Longnecker R. 2018. Ephrin receptor A2 is a functional entry receptor for Epstein-Barr virus. *Nat*
601 *Microbiol* 3:172–180.

602 17. Chen J, Zhang X, Schaller S, Jardetzky TS, Longnecker R. 2019. Ephrin Receptor A4 is a
603 New Kaposi's Sarcoma-Associated Herpesvirus Virus Entry Receptor. *mBio* 10:e02892-18.

604 18. Großkopf AK, Schlagowski S, Fricke T, Ensser A, Desrosiers RC, Hahn AS. 2021. P1xdc
605 family members are novel receptors for the rhesus monkey rhadinovirus (RRV). *PLoS Pathog*
606 17:e1008979.

607 19. Hahn AS, Kaufmann JK, Wies E, Naschberger E, Panteleev-Ivlev J, Schmidt K, Holzer
608 A, Schmidt M, Chen J, König S, Ensser A, Myoung J, Brockmeyer NH, Stürzl M, Fleckenstein
609 B, Neipel F. 2012. The ephrin receptor tyrosine kinase A2 is a cellular receptor for Kaposi's
610 sarcoma-associated herpesvirus. *Nat Med* 18:961–966.

611 20. Chakraborty S, Valiyaveettil M, Sadagopan S, Paudel N, Chandran B. 2011. c-Cbl-
612 Mediated Selective Virus-Receptor Translocations into Lipid Rafts Regulate Productive Kaposi's
613 Sarcoma-Associated Herpesvirus Infection in Endothelial Cells. *J Virol* 85:12410–12430.

614 21. Dutta D, Chakraborty S, Bandyopadhyay C, Valiya Veettil M, Ansari MA, Singh VV,
615 Chandran B. 2013. EphrinA2 Regulates Clathrin Mediated KSHV Endocytosis in Fibroblast
616 Cells by Coordinating Integrin-Associated Signaling and c-Cbl Directed Polyubiquitination.
617 *PLoS Pathog* 9:e1003510.

618 22. Kaleeba JAR, Berger EA. 2006. Kaposi's Sarcoma-Associated Herpesvirus Fusion-Entry
619 Receptor: Cystine Transporter xCT. *Science* 311:1921–1924.

620 23. Raab MS, Albrecht JC, Birkmann A, Yağuboğlu S, Lang D, Fleckenstein B, Neipel F.
621 1998. The immunogenic glycoprotein gp35-37 of human herpesvirus 8 is encoded by open
622 reading frame K8.1. *J Virol* 72:6725–6731.

623 24. Birkmann A, Mahr K, Ensser A, Yağuboğlu S, Titgemeyer F, Fleckenstein B, Neipel F.
624 2001. Cell Surface Heparan Sulfate Is a Receptor for Human Herpesvirus 8 and Interacts with
625 Envelope Glycoprotein K8.1. *Journal of Virology* 75:11583–11593.

626 25. Dollery SJ, Santiago-Crespo RJ, Chatterjee D, Berger EA. 2018. Glycoprotein K8.1A of
627 Kaposi's sarcoma-associated herpesvirus is a critical B cell tropism determinant, independent of
628 its heparan sulfate binding activity. *J Virol* <https://doi.org/10.1128/JVI.01876-18>.

- 629 26. Haan KM, Kyeong Lee S, Longnecker R. 2001. Different Functional Domains in the
630 Cytoplasmic Tail of Glycoprotein B Are Involved in Epstein–Barr Virus-Induced Membrane
631 Fusion. *Virology* 290:106–114.
- 632 27. Bruce AG, Ryan JT, Thomas MJ, Peng X, Grundhoff A, Tsai C-C, Rose TM. 2013. Next-
633 generation sequence analysis of the genome of RFHVMn, the macaque homolog of Kaposi’s
634 sarcoma (KS)-associated herpesvirus, from a KS-like tumor of a pig-tailed macaque. *J Virol*
635 87:13676–13693.
- 636 28. Steentoft C, Vakhrushev SY, Joshi HJ, Kong Y, Vester-Christensen MB, Schjoldager KT-
637 BG, Lavrsen K, Dabelsteen S, Pedersen NB, Marcos-Silva L, Gupta R, Bennett EP, Mandel U,
638 Brunak S, Wandall HH, Lavery SB, Clausen H. 2013. Precision mapping of the human O-
639 GalNAc glycoproteome through SimpleCell technology. *EMBO J* 32:1478–1488.
- 640 29. Luna RE, Zhou F, Baghian A, Chouljenko V, Forghani B, Gao S-J, Kousoulas KG. 2004.
641 Kaposi’s Sarcoma-Associated Herpesvirus Glycoprotein K8.1 Is Dispensable for Virus Entry.
642 *Journal of Virology* 78:6389–6398.
- 643 30. Wu L, Renne R, Ganem D, Forghani B. 2000. Human herpesvirus 8 glycoprotein K8.1:
644 expression, post-translational modification and localization analyzed by monoclonal antibody. *J*
645 *Clin Virol* 17:127–136.
- 646 31. Zhu L, Puri V, Chandran B. 1999. Characterization of Human Herpesvirus-8 K8.1A/B
647 Glycoproteins by Monoclonal Antibodies. *Virology* 262:237–249.
- 648 32. Stürzl M, Gaus D, Dirks WG, Ganem D, Jochmann R. 2013. Kaposi’s sarcoma-derived
649 cell line SLK is not of endothelial origin, but is a contaminant from a known renal carcinoma cell
650 line. *Int J Cancer* 132:1954–1958.
- 651 33. Genberg M, Mark J, Hakelius L, Ericsson J, Nistér M. 1989. Origin and relationship
652 between different cell types in malignant fibrous histiocytoma. *Am J Pathol* 135:1185–1196.
- 653 34. Deyrieux AF, Wilson VG. 2007. In vitro culture conditions to study keratinocyte
654 differentiation using the HaCaT cell line. *Cytotechnology* 54:77–83.
- 655 35. Reed JA, Nador RG, Spaulding D, Tani Y, Cesarman E, Knowles DM. 1998.
656 Demonstration of Kaposi’s sarcoma-associated herpes virus cyclin D homolog in cutaneous
657 Kaposi’s sarcoma by colorimetric in situ hybridization using a catalyzed signal amplification
658 system. *Blood* 91:3825–3832.
- 659 36. Cerimele F, Curreli F, Ely S, Friedman-Kien AE, Cesarman E, Flore O. 2001. Kaposi’s
660 sarcoma-associated herpesvirus can productively infect primary human keratinocytes and alter
661 their growth properties. *J Virol* 75:2435–2443.
- 662 37. Foreman KE, Bacon PE, Hsi ED, Nickoloff BJ. 1997. In situ polymerase chain reaction-
663 based localization studies support role of human herpesvirus-8 as the cause of two AIDS-related
664 neoplasms: Kaposi’s sarcoma and body cavity lymphoma. *J Clin Invest* 99:2971–2978.
- 665 38. Boukamp P, Petrussevska RT, Breitkreutz D, Hornung J, Markham A, Fusenig NE. 1988.
666 Normal keratinization in a spontaneously immortalized aneuploid human keratinocyte cell line. *J*
667 *Cell Biol* 106:761–771.
- 668 39. Großkopf AK, Schlagowski S, Hörnich BF, Fricke T, Desrosiers RC, Hahn AS. 2019.
669 EphA7 Functions as Receptor on BJAB Cells for Cell-to-Cell Transmission of the Kaposi’s
670 Sarcoma-Associated Herpesvirus and for Cell-Free Infection by the Related Rhesus Monkey
671 Rhadinovirus. *J Virol* 93:e00064-19.
- 672 40. Magrath IT, Freeman CB, Pizzo P, Gadek J, Jaffe E, Santaella M, Hammer C, Frank M,
673 Reaman G, Novikovs L. 1980. Characterization of lymphoma-derived cell lines: comparison of
674 cell lines positive and negative for Epstein-Barr virus nuclear antigen. II. Surface markers. *J Natl*
675 *Cancer Inst* 64:477–483.
- 676 41. O’Connor PM, Wassermann K, Sarang M, Magrath I, Bohr VA, Kohn KW. 1991.

677 Relationship between DNA cross-links, cell cycle, and apoptosis in Burkitt's lymphoma cell lines
678 differing in sensitivity to nitrogen mustard. *Cancer Res* 51:6550–6557.

679 42. Menezes J, Leibold W, Klein G, Clements G. 1975. Establishment and characterization of
680 an Epstein-Barr virus (EBV)-negative lymphoblastoid B cell line (BJA-B) from an exceptional,
681 EBV-genome-negative African Burkitt's lymphoma. *Biomedicine* 22:276–284.

682 43. Pulvertaft JV. 1964. CYTOLOGY OF BURKITT'S TUMOUR (AFRICAN
683 LYMPHOMA). *Lancet* 1:238–240.

684 44. Hampar B, Derge JG, Martos LM, Walker JL. 1972. Synthesis of Epstein-Barr virus after
685 activation of the viral genome in a "virus-negative" human lymphoblastoid cell (Raji) made
686 resistant to 5-bromodeoxyuridine (thymidine kinase-virus antigen-immunofluorescence-
687 herpesvirus fingerprints). *Proc Natl Acad Sci U S A* 69:78–82.

688 45. Dollery SJ, Santiago-Crespo RJ, Kardava L, Moir S, Berger EA. 2014. Efficient infection
689 of a human B cell line with cell-free Kaposi's sarcoma-associated herpesvirus. *J Virol* 88:1748–
690 1757.

691 46. Myoung J, Ganem D. 2011. Infection of Lymphoblastoid Cell Lines by Kaposi's
692 Sarcoma-Associated Herpesvirus: Critical Role of Cell-Associated Virus. *Journal of Virology*
693 85:9767–9777.

694 47. Hahn A, Birkmann A, Wies E, Dorer D, Mahr K, Stürzl M, Titgemeyer F, Neipel F. 2009.
695 Kaposi's sarcoma-associated herpesvirus gH/gL: glycoprotein export and interaction with cellular
696 receptors. *J Virol* 83:396–407.

697 48. Hahn AS, Desrosiers RC. 2013. Rhesus Monkey Rhadinovirus Uses Eph Family
698 Receptors for Entry into B Cells and Endothelial Cells but Not Fibroblasts. *PLOS Pathogens*
699 9:e1003360.

700 49. Rappocciolo G, Jenkins FJ, Hensler HR, Piazza P, Jais M, Borowski L, Watkins SC,
701 Rinaldo CR. 2006. DC-SIGN Is a Receptor for Human Herpesvirus 8 on Dendritic Cells and
702 Macrophages. *J Immunol* 176:1741–1749.

703 50. TerBush AA, Hafkamp F, Lee HJ, Coscoy L. 2018. A Kaposi's Sarcoma-Associated
704 Herpesvirus Infection Mechanism is Independent of Integrins $\alpha 3\beta 1$, $\alpha V\beta 3$, and $\alpha V\beta 5$. *J Virol*
705 <https://doi.org/10.1128/JVI.00803-18>.

706 51. Hörnich BF, Großkopf AK, Dcosta CJ, Schlagowski S, Hahn AS. 2021. Interferon-
707 Induced Transmembrane Proteins Inhibit Infection by the Kaposi's Sarcoma-Associated
708 Herpesvirus and the Related Rhesus Monkey Rhadinovirus in a Cell-Specific Manner. *mBio*
709 12:e0211321.

710 52. Fricke T, Großkopf AK, Ensser A, Backovic M, Hahn AS. 2022. Antibodies Targeting
711 KSHV gH/gL Reveal Distinct Neutralization Mechanisms. 3. *Viruses* 14:541.

712 53. Colombo I, Sangiovanni E, Maggio R, Mattozzi C, Zava S, Corbett Y, Fumagalli M,
713 Carlino C, Corsetto PA, Scaccabarozzi D, Calvieri S, Gismondi A, Taramelli D, Dell'Agli M.
714 2017. HaCaT Cells as a Reliable In Vitro Differentiation Model to Dissect the
715 Inflammatory/Repair Response of Human Keratinocytes. *Mediators Inflamm* 2017:7435621.

716 54. Hayes AJ, Melrose J. 2023. HS, an Ancient Molecular Recognition and Information
717 Storage Glycosaminoglycan, Equips HS-Proteoglycans with Diverse Matrix and Cell-Interactive
718 Properties Operative in Tissue Development and Tissue Function in Health and Disease. 2.
719 *International Journal of Molecular Sciences* 24:1148.

720 55. Tanner J, Weis J, Fearon D, Whang Y, Kieff E. 1987. Epstein-Barr virus gp350/220
721 binding to the B lymphocyte C3d receptor mediates adsorption, capping, and endocytosis. *Cell*
722 50:203–213.

723 56. Brulois KF, Chang H, Lee AS-Y, Ensser A, Wong L-Y, Toth Z, Lee SH, Lee H-R,
724 Myoung J, Ganem D, Oh T-K, Kim JF, Gao S-J, Jung JU. 2012. Construction and Manipulation

725 of a New Kaposi's Sarcoma-Associated Herpesvirus Bacterial Artificial Chromosome Clone.
726 *Journal of Virology* 86:9708–9720.

727 57. Myoung J, Ganem D. 2011. Generation of a doxycycline-inducible KSHV producer cell
728 line of endothelial origin: Maintenance of tight latency with efficient reactivation upon induction.
729 *Journal of Virological Methods* 174:12–21.

730 58. Tischer BK, von Einem J, Kaufer B, Osterrieder N. 2006. Two-step red-mediated
731 recombination for versatile high-efficiency markerless DNA manipulation in *Escherichia coli*.
732 *BioTechniques* 40:191–197.

733 59. Großkopf AK, Ensser A, Neipel F, Jungnickl D, Schlagowski S, Desrosiers RC, Hahn AS.
734 2018. A conserved Eph family receptor-binding motif on the gH/gL complex of Kaposi's
735 sarcoma-associated herpesvirus and rhesus monkey rhadinovirus. *PLoS Pathog* 14:e1006912.

736 60. Lang D, Birkmann A, Neipel F, Hinderer W, Rothe M, Ernst M, Sonneborn HH. 2000.
737 Generation of monoclonal antibodies directed against the immunogenic glycoprotein K8.1 of
738 human herpesvirus 8. *Hybridoma* 19:287–295.

739 61. Hörnich BF, Großkopf AK, Schlagowski S, Tenbusch M, Kleine-Weber H, Neipel F,
740 Stahl-Hennig C, Hahn AS. 2021. SARS-CoV-2 and SARS-CoV Spike-Mediated Cell-Cell
741 Fusion Differ in Their Requirements for Receptor Expression and Proteolytic Activation. *J Virol*
742 95:e00002-21.

743 62. Niwa H, Yamamura K, Miyazaki J. 1991. Efficient selection for high-expression
744 transfectants with a novel eukaryotic vector. *Gene* 108:193–199.

745